

Minerva Access is the Institutional Repository of The University of Melbourne

Author/s:

Shanley, HT;Taki, AC;Byrne, JJ;Jabbar, A;Wells, TNC;Samby, K;Boag, PR;Nguyen, N;Sleeb, BE;Gasser, RB

Title:

A High-Throughput Phenotypic Screen of the 'Pandemic Response Box' Identifies a Quinoline Derivative with Significant Anthelmintic Activity

Date:

2022-02-01

Citation:

Shanley, H. T., Taki, A. C., Byrne, J. J., Jabbar, A., Wells, T. N. C., Samby, K., Boag, P. R., Nguyen, N., Sleeb, B. E. & Gasser, R. B. (2022). A High-Throughput Phenotypic Screen of the 'Pandemic Response Box' Identifies a Quinoline Derivative with Significant Anthelmintic Activity. *Pharmaceuticals*, 15 (2), <https://doi.org/10.3390/ph15020257>.

Persistent Link:



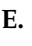

<https://hdl.handle.net/11343/302671>

License:

CC BY

Article

A High-Throughput Phenotypic Screen of the ‘Pandemic Response Box’ Identifies a Quinoline Derivative with Significant Anthelmintic Activity

Harrison T. Shanley ¹, Aya C. Taki ¹, Joseph J. Byrne ¹, Abdul Jabbar ¹, Tim N. C. Wells ², Kirandeep Samby ², Peter R. Boag ³, Nghi Nguyen ⁴, Brad E. Sleebs ⁴ and Robin B. Gasser ^{1,*}

- ¹ Department of Veterinary Biosciences, Faculty of Veterinary and Agricultural Sciences, The University of Melbourne, Parkville, VIC 3010, Australia; hshanley@student.unimelb.edu.au (H.T.S.); aya.taki@unimelb.edu.au (A.C.T.); byrnej1@unimelb.edu.au (J.J.B.); jabbara@unimelb.edu.au (A.J.)
- ² Medicines for Malaria Venture (MMV), 1215 Geneva, Switzerland; wellst@mmv.org (T.N.C.W.); sambyk-consultants@mmv.org (K.S.)
- ³ Monash Biomedicine Discovery Institute, Department of Biochemistry and Molecular Biology, Monash University, Clayton, VIC 3800, Australia; peter.boag@monash.edu
- ⁴ Chemical Biology Division, The Walter and Eliza Hall Institute of Medical Research, Parkville, VIC 3052, Australia; nguyen.n@wehi.edu.au (N.N.); sleebs@wehi.edu.au (B.E.S.)
- * Correspondence: robinbg@unimelb.edu.au



Citation: Shanley, H.T.; Taki, A.C.; Byrne, J.J.; Jabbar, A.; Wells, T.N.C.; Samby, K.; Boag, P.R.; Nguyen, N.; Sleebs, B.E.; Gasser, R.B. A High-Throughput Phenotypic Screen of the ‘Pandemic Response Box’ Identifies a Quinoline Derivative with Significant Anthelmintic Activity. *Pharmaceuticals* **2022**, *15*, 257. <https://doi.org/10.3390/ph15020257>

Academic Editors: Jean Leandro dos Santos and Chung Man Chin

Received: 3 February 2022

Accepted: 18 February 2022

Published: 21 February 2022

Publisher’s Note: MDPI stays neutral with regard to jurisdictional claims in published maps and institutional affiliations.



Copyright: © 2022 by the authors. Licensee MDPI, Basel, Switzerland. This article is an open access article distributed under the terms and conditions of the Creative Commons Attribution (CC BY) license (<https://creativecommons.org/licenses/by/4.0/>).

Abstract: Parasitic nematodes cause diseases in livestock animals and major economic losses to the agricultural industry worldwide. Nematodes of the order Strongylida, including *Haemonchus contortus*, are particularly important. The excessive use of anthelmintic compounds to treat infections and disease has led to widespread resistance to these compounds in nematodes, such that there is a need for new anthelmintics with distinctive mechanisms of action. With a focus on discovering new anthelmintic entities, we screened 400 chemically diverse compounds within the ‘Pandemic Response Box’ (from Medicines for Malaria Venture, MMV) for activity against *H. contortus* and its free-living relative, *Caenorhabditis elegans*—a model organism. Using established phenotypic assays, test compounds were evaluated in vitro for their ability to inhibit the motility and/or development of *H. contortus* and *C. elegans*. Dose-response evaluations identified a compound, MMV1581032, that significantly the motility of *H. contortus* larvae ($IC_{50} = 3.4 \pm 1.1 \mu M$) and young adults of *C. elegans* ($IC_{50} = 7.1 \pm 4.6 \mu M$), and the development of *H. contortus* larvae ($IC_{50} = 2.2 \pm 0.7 \mu M$). The favourable characteristics of MMV1581032, such as suitable physicochemical properties and an efficient, cost-effective pathway to analogue synthesis, indicates a promising candidate for further evaluation as a nematocide. Future work will focus on a structure-activity relationship investigation of this chemical scaffold, a toxicity assessment of potent analogues and a mechanism/mode of action investigation.

Keywords: *Haemonchus contortus*; parasitic nematode; *Caenorhabditis elegans*; anthelmintics; small molecules; *Pandemic Response Box*; phenotypic screening

1. Introduction

Parasitic roundworms (nematodes) cause infections and diseases (nematodiasis) in humans and animals that have a major adverse socioeconomic impact worldwide [1,2]. In humans, nematodiasis disproportionately affect poverty-stricken communities, with hookworm disease, ascariasis, trichuriasis and strongyloidiasis, for example, being classified by the World Health Organization (WHO) as some of the most neglected tropical diseases [3]. From a global, agricultural perspective, productivity losses in livestock animals caused by nematodes are estimated at tens of billions of dollars [4]. Most losses in these animals relate to nematodes (order Strongylida) of the gastrointestinal and respiratory tracts. One key representative is *Haemonchus contortus* (family Trichostrongylidae), also known as the ‘barber’s pole worm’, which causes haemonchosis—a disease of ruminant livestock, such

as sheep and goats. Haemonchosis is characterised by anaemia, bottle jaw, lethargy, poor wool/milk production and/or sudden death [5,6]. *H. contortus* is transmitted orally via a direct life cycle [7]; animals become infected by ingesting infective third-stage larvae (L3s), which exsheath in the forestomachs and develop, via fourth-stage larvae (L4s), to dioecious blood-feeding adult worms in the abomasum, where they reproduce, with females releasing eggs via faeces into the environment [7].

Treatment with anthelmintic compounds is an important component of the control of trichostrongyloid nematodes [8]. Compound classes include benzimidazoles, imidazothiazoles, macrocyclic lactones, salicylanilides, amino-acetonitrile derivatives and spiroindoles, which are commercially available to combat parasitic nematodes, including *H. contortus* [6,9]. However, the excessive and frequent use of these compounds has led to widespread resistance (including multidrug resistance) to all available classes, with the exception of the spiroindole derquantel [10,11]. Resistance develops rapidly, usually emerging within 5–10 years following the introduction of a compound on to the commercial market [12,13]. Whilst non-chemotherapeutic methods of parasite control, such as grazing management, biological control or vaccination, could prevent anthelmintic resistance, no such method appears to be highly effective without the complementary use of anthelmintic compounds [6,14].

Although the rate of discovery and development of novel anthelmintics has been relatively slow, with only monepantel [15] and derquantel [16,17] entering the commercial market since 2009, there is an impetus to discover novel chemotherapeutics with mechanisms of action against parasitic nematodes that differ from those currently commercially available. Recent progress using moderate- to high-throughput, whole-parasite screening assays has enabled the discovery of a range of synthetic and natural compounds with anthelmintic activity (reviewed by [18,19]). This progress has been enabled by the availability of diverse, well-curated compound libraries from philanthropic and commercial partners, including Compounds Australia (Griffith Institute for Drug Discovery, Australia), Johnson & Johnson and Medicines for Malaria Venture (MMV; Geneva, Switzerland) [18,20–31]. Some previous work, in collaboration with MMV, identified an approved pesticide (tolfenpyrad) and two kinase inhibitors (SNS-032 and AG-1295) with anthelmintic activity against *H. contortus* within the *Pathogen* ($n = 400$ compounds) and *Stasis* ($n = 400$ compounds) Box' collections. Both tolfenpyrad and AG-1295 underwent chemical optimisation, structure-activity relationship (SAR) and/or toxicity studies, although a safe lead compound was not attained [27,32,33]. To continue the pursuit of a new and effective anthelmintic entity, we extend our discovery effort, together with MMV. We sourced the newly assembled 'Pandemic Response Box', which contains 400 structurally diverse and well-curated compounds with activities against key pathogenic bacteria ($n = 201$ entities), fungi ($n = 46$) and viruses ($n = 153$), including highly significant pathogens, such as the bacterium *Staphylococcus aureus* and the virus Influenza A.

In addition to the availability of chemical libraries through collaborations with organisations such as MMV, progress in 'multi-omics' research has complemented anthelmintic drug discovery—with significant advances in the understanding of the *H. contortus* genome, transcriptome, proteome and lipidome [34–43]. The use of these multi-omics advances provides a promising pathway to elucidate the mechanisms of action of novel anthelmintic compounds in *H. contortus*. In addition, the closely related free-living nematode, *Caenorhabditis elegans*, provides a powerful comparator for such mechanistic studies [44–46]. The genome and transcriptome of *C. elegans* has been comprehensively annotated and made publicly available from WormBase (www.wormbase.org [47]; accessed on 15 September 2021). Despite being a free-living nematode, *C. elegans* belongs to the same evolutionary clade (V) as *H. contortus*, with these two species sharing 7361 one-to-one orthologous genes [34,35,39,48]. *C. elegans* is a powerful surrogate for *H. contortus* and can be used to infer the functions of orthologous gene or protein targets [45,46,48]. Hence, the identification of novel anthelmintic compounds via high-throughput screening, complemented

with these tools for elucidating mode(s) of action, creates a pathway toward anthelmintic drug discovery.

Here, we (i) undertook a whole-organism, phenotypic primary screen of compounds from the *Pandemic Response Box* against *H. contortus* and *C. elegans* to identify active compounds; (ii) assessed the potency of anthelmintic activity of (hit) compounds; and (iii) evaluated the toxicity of these hit compounds against HepG2 cells, in order to identify candidate compounds for medicinal chemistry optimisation.

2. Results

2.1. Primary Screen Identifies Three Compounds with Anthelmintic Activity

Two compounds (Figure 1a) had marked activity and induced phenotypic changes in *H. contortus* xL3s: MMV1581032 reduced xL3 motility by $\geq 100\%$ at 90 h, inhibited larval development and induced a ‘straight’ (*Str*) phenotype after seven days; MMV1593539 reduced larval motility by 66%, inhibited larval development and also induced a *Str* phenotype. Two compounds had marked activity on *C. elegans* in the transition from the L4 to the adult stage (Figure 1b): MMV1581032 and MMV1593515 inhibited larval motility by 90% and 66%, respectively, at 40 h. Thus, MMV1581032 reduced the motility of both *H. contortus* and *C. elegans* at a concentration of 20 μM . Throughout the primary screen, the Z' -factor was consistently between 0.74 and 0.86.

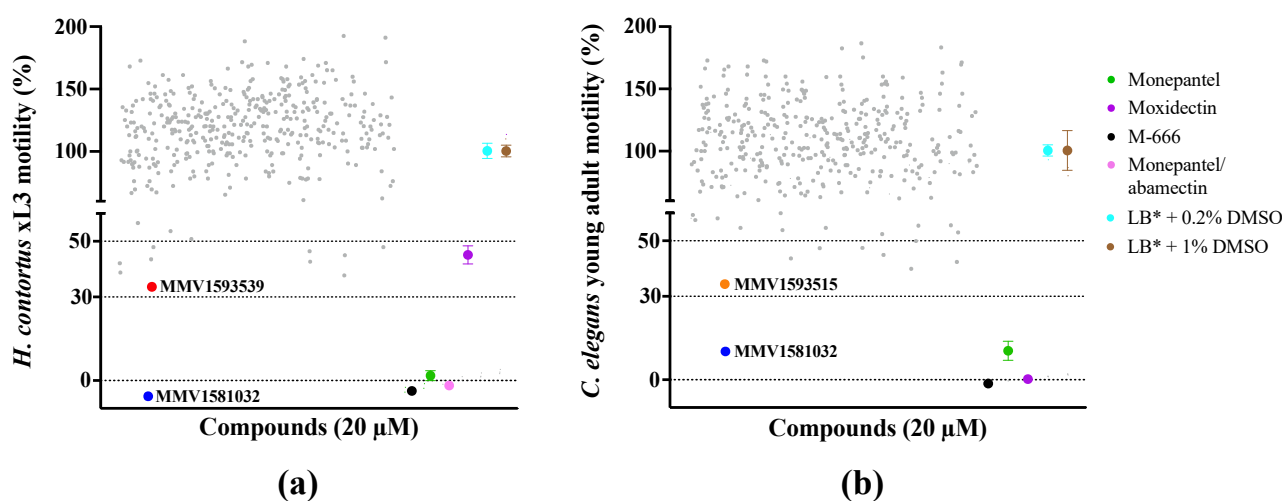


Figure 1. Results of the primary screen of the Medicines for Malaria Venture (MMV) *Pandemic Response Box* ($n = 400$) against (a) exsheathed third-stage larvae (xL3s) of *Haemonchus contortus* and (b) young adults of *Caenorhabditis elegans* with reference to four distinct control compounds (monepantel, moxidectin, M-666 and monepantel/abamectin) and negative (LB* + DMSO only) controls. All test and positive control compounds were tested at 20 μM . Each grey dot represents an individual test compound. Mean \pm standard error of the mean (SEM) indicated for negative and positive control compounds (four data points for each positive control; 24 data points for LB* + 0.2% DMSO; eight data points for LB* + 1% DMSO).

2.2. Potency and Toxicity Assessments Reveal One Promising Anthelmintic Candidate

An assessment of the potency of two hit compounds to inhibit the motility of *H. contortus* xL3s was estimated following incubation for 90 h (Figure 2a; Table 1). Compound MMV1581032 displayed a half-maximal inhibitory concentration (IC_{50}) of $3.4 \pm 1.1 \mu\text{M}$ (maximum motility inhibition: 76%) and compound MMV1593539 had an IC_{50} of $3.5 \pm 0.98 \mu\text{M}$ (maximum motility inhibition: 71%)—being comparable to that of moxidectin ($\text{IC}_{50} = 7.4 \pm 4.2 \mu\text{M}$; maximum motility inhibition: 70%) in the present dose-response assay. Subsequently, the potency of each compound to inhibit larval development of *H. contortus* was assessed following incubation for seven days (Figure 2b; Table 1). MMV1581032 displayed an IC_{50} of $2.2 \pm 0.68 \mu\text{M}$, and MMV1593539 achieved an IC_{50}

of $1.3 \pm 0.11 \mu\text{M}$, values that were comparable to that of moxidectin ($\text{IC}_{50} = 2.4 \mu\text{M}$). MMV1581032 was also evaluated for motility inhibition on adult females of *H. contortus* (Figure 3). MMV1581032 reduced the motility of these worms by ~0%, 22%, 33%, 63% and 100% over the time course of 1 h, 2 h, 3 h, 5 h and 24 h, respectively. Respective values for monepantel and moxidectin (Figure 3) were: 22% and 67% at 1 h; 22% and 67% at 2 h; 33% and 75% at 3 h; 43% and 72% at 5 h; and 100% and 72% at 24 h.

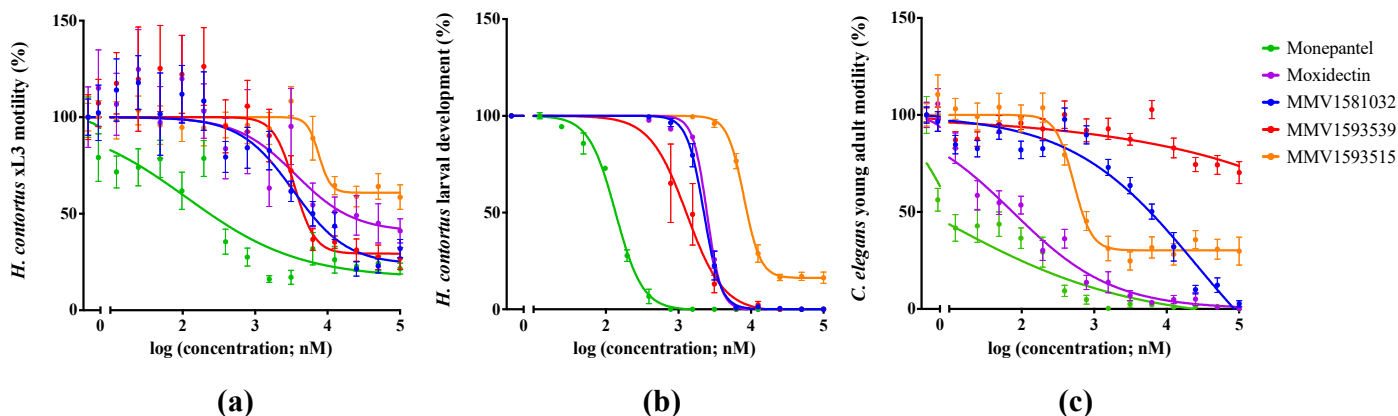


Figure 2. The potencies of three active test compounds (MMV1581032, MMV1593539 and MMV1593515) against exsheathed third-stage larvae (xL3s) of *Haemonchus contortus* and young adults of *Caenorhabditis elegans* with reference to two control compounds (monepantel and moxidectin). Dose-response curves show (a) the inhibition of *H. contortus* motility at 90 h, (b) the inhibition of *H. contortus* development at seven days and (c) the reduction of *C. elegans* motility at 40 h. Data points represent three independent experiments conducted in triplicate; the mean \pm standard error of the mean (SEM).

Table 1. Summary of the potency assessment of hit compounds and positive control compounds (monepantel and moxidectin) on *Haemonchus contortus* and *Caenorhabditis elegans*.

Compound.	<i>H. contortus</i>			<i>C. elegans</i>
	Larval Motility (90 h) $\text{IC}_{50} \pm \text{SD} (\mu\text{M})$	Larval Development (168 h) $\text{IC}_{50} \pm \text{SD} (\mu\text{M})$	Abnormal Phenotype (168 h)	Young Adult Motility (40 h) $\text{IC}_{50} \pm \text{SD} (\mu\text{M})$
MMV1581032	3.4 ± 1.1 (76)	2.2 ± 0.7	<i>Str</i>	7.1 ± 4.6 (96)
MMV1593539	3.5 ± 0.98 (71)	1.3 ± 0.1	<i>Str</i>	>100
MMV1593515	7.6 ± 2.9 (38)	8.0 ± 0.87	–	0.5 ± 0.02 (75)
Monepantel	0.11 ± 0.003 (84)	0.013 ± 0.002	<i>Coi</i>	0.01 ± 0.002 (100)
Moxidectin	7.4 ± 4.2 (70)	2.4 ± 0.01	<i>Cur</i>	0.04 ± 0.0004 (100)

IC_{50} calculated from three independent assays conducted in triplicate. Value in parentheses represents the maximum motility inhibition (%). *Str*, straight; –, no apparent distinction from wild-type, but reduced motility; *Coi*, coiled; *Cur*, curved.

An assessment of the potency of two hit compounds to inhibit the motility of *C. elegans* was estimated following incubation for 40 h (Figure 2c; Table 1): MMV1581032 exhibited an IC_{50} of $7.1 \pm 4.6 \mu\text{M}$ (maximum motility inhibition: 96%). MMV1593515 achieved an IC_{50} value of $0.5 \pm 0.11 \mu\text{M}$ (maximum motility inhibition: 75%). Respective IC_{50} values for monepantel and moxidectin were $0.01 \pm 2.0 \times 10^{-3} \mu\text{M}$ and $0.04 \pm 4.0 \times 10^{-4} \mu\text{M}$. Thus, MMV1581032 exhibited marked potency against both *H. contortus* and *C. elegans*.

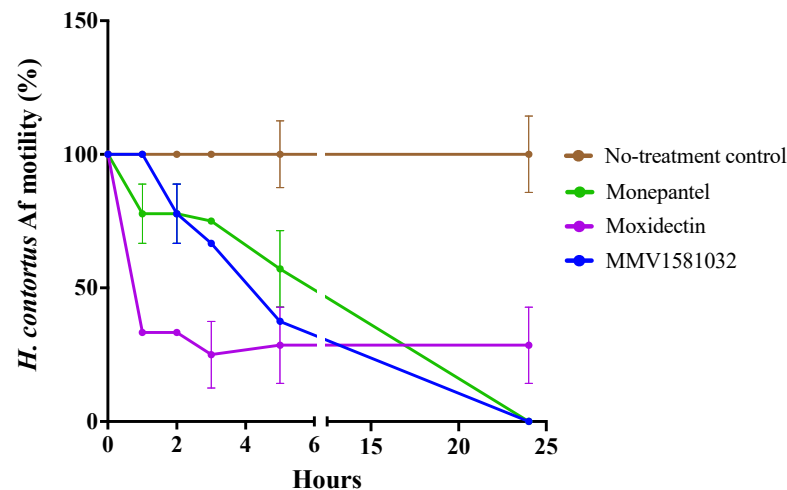


Figure 3. In vitro motility inhibition (%) of MMV1581032 on adult females of *Haemonchus contortus* with reference to two control compounds (monepantel and moxidectin) over a period of 24 h. Motility scores (assessed at 1-, 2-, 3-, 5- and 24-h time points; cf. [29]) for each compound were calculated, normalised with reference to the negative control (100% motility) and were recorded as a percentage. Data points represent one experiment conducted in triplicate; mean \pm standard deviation (SD).

Given the potential of MMV1581032 as a candidate, its toxicity was assessed by measuring cell death using crystal violet staining (Figure 4). This compound was shown to be neither cytotoxic ($CC_{50} \geq 100 \mu\text{M}$) nor mitotoxic ($MC_{50} = 81.1 \mu\text{M}$) against HepG2 human hepatoma cells.

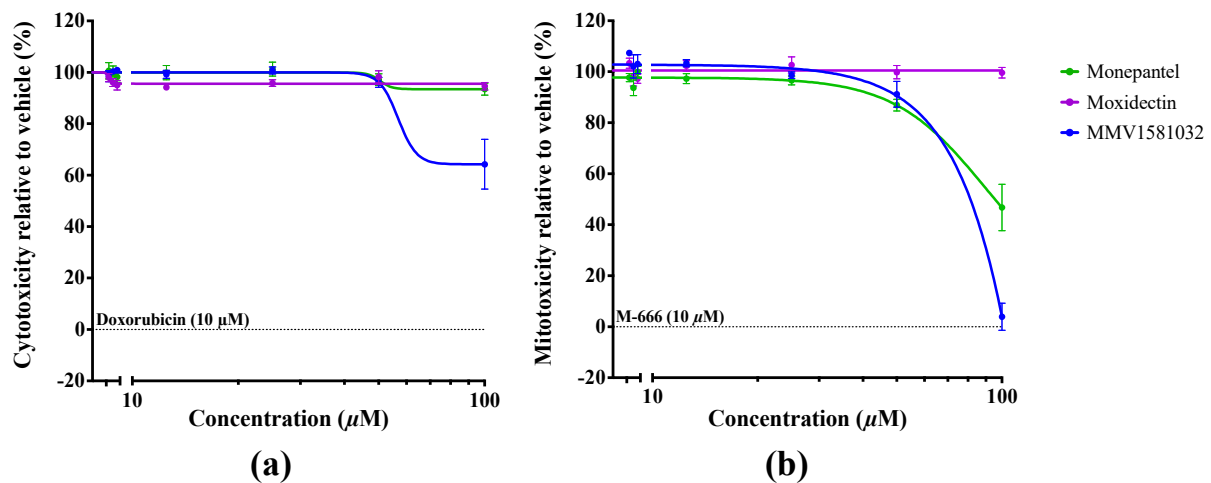


Figure 4. Toxicity assessment of MMV1581032, moxidectin and monepantel on HepG2 human hepatoma cells with reference to two positive controls; doxorubicin (cytotoxic) and M-666 (mitotoxic). A cell-viability assay was employed to estimate (a) the half-maximal cytotoxic concentration (CC_{50}) and (b) the half-maximal mitotoxic concentration (MC_{50}) after 48 h of incubation with compound. Crystal violet staining was utilised to measure the absorbance (595 nm) of treated cells compared to the negative control (100% cell viability) and baseline-corrected using respective positive controls. Data points represent one experiment conducted in triplicate; mean \pm standard error of the mean (SEM).

3. Discussion

The screening of 400 diverse, drug-like molecules identified three compounds (Figure 5), designated as MMV1593539, MMV1593515 and MMV1581032, with anthelmintic activity against *H. contortus* and/or *C. elegans*. MMV1581032 was shown to be the most potent of these compounds against both *H. contortus* and *C. elegans*, with IC_{50} values of $3.4 \mu\text{M}$ and

7.1 μM , respectively, and killed adult females of *H. contortus* at 100 μM in vitro after 24 h. Thus, MMV1581032 presented as a suitable candidate for further evaluation.

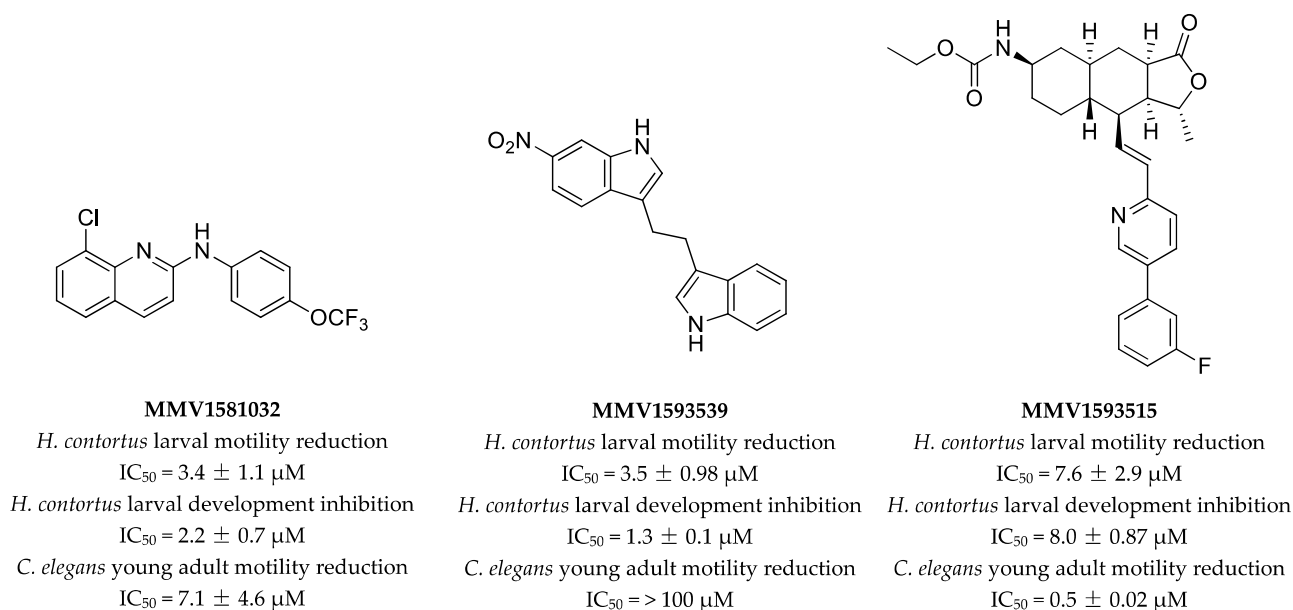


Figure 5. Chemical structures of MMV1581032, MMV1593539 and MMV1593515. Half of the maximum inhibitory concentration (IC_{50}) values of each compound were established for the inhibition of *H. contortus* larval motility at 90 h, the inhibition of larval development of *H. contortus* at seven days and the reduction of motility of young adults of *C. elegans* at 40 h. The IC_{50} values are presented as mean \pm standard deviation. Three independent assays were conducted in triplicate.

Compound MMV1593539—a bis-indole derivative—was shown to be potent against *H. contortus* (3.5 μM) but not *C. elegans* (>100 μM). The reduction in both larval motility and development of *H. contortus* was comparable with that of moxidectin, but less than that of monepantel. MMV1593539 induced a ‘straight’ (*Str*) phenotype in *H. contortus* xL3s at 100 μM —a phenotype induced by other compounds, such as tolfenpyrad—a pyrazole-5-carboxamide [23]—and goniothalamin—an α -pyrone [49]. Zoraghi et al. [50] first reported MMV1593539 as a pyruvate kinase inhibitor that is selective against *Staphylococcus aureus*. Notably, genes encoding pyruvate kinase (codes HCON_00010565, HCON_00010570 and HCON_00010580; ref. [39]) have been identified in *H. contortus*. Although compound MMV1593539 is selective for pyruvate kinase in *S. aureus*, it is not clear whether this is the case in *H. contortus*. However, as MMV1593539 did not show activity against *C. elegans*, the ability to perform mechanism of action studies in the N2 strain of this free-living nematode as a tool might be limited. However, other strains of *C. elegans* which are more sensitive to drugs, such as *bus-2* [51], might be more applicable. As the bis-indole structure of MMV1593539 is metabolically labile [52] and nitro functional groups (bis-amine reduction) are often associated with toxicity issues [53], the compound is not favourable from a medicinal chemistry perspective. Therefore, despite its potent anthelmintic activity against *H. contortus* larvae, SAR studies may not yield a promising lead candidate.

Compound MMV1593515—a natural himbacine derivative, also known as vorapaxar [54]—displayed a low potency (maximum motility inhibition of 38% at 7.6 μM) against *H. contortus* xL3s but high potency (0.5 μM) against *C. elegans*. Vorapaxar, an anti-platelet drug (PAR-1 antagonist), was first described in 2008 and is currently commercially available as Zontivity[®] for the treatment of people with a history of heart attacks [54,55]. Interestingly, himbacine derivatives have been identified previously as human muscarinic acetylcholine receptor antagonists [56,57]. In *C. elegans*, the human muscarinic receptor ortholog, GAR-3, has been implicated in the regulation of muscle contraction [58]—thus, it is proposed that GAR-3 antagonism by MMV1593515 is responsible for motility reduction

in *C. elegans*, although a mode of action study would be needed to test this hypothesis. Despite the low potency against *H. contortus*, voraxapar might exert anthelmintic activity against other socioeconomically important parasitic nematodes of the order Strongylida (e.g., species of *Ostertagia*, *Teladorsagia*, *Trichostrongylus*, *Cooperia* and/or *Ancylostoma*), given the promising potency against *C. elegans*, which is within the same evolutionary clade (V) as the Strongylida [59,60]. However, an SAR investigation utilising MMV1593515 should consider the challenges associated with producing himbacine-derivatives. As synthesising the himbacine core requires a complex multi-step (>10 steps) process [54,56,61–63], synthesising MMV1593515 analogues would likely be costly and time-consuming, important factors to consider prior to embarking on medicinal chemistry optimisation.

Compound MMV1581032—a quinoline derivative, also known as “ABX464” (cf. [64,65])—affected motility (*H. contortus* and *C. elegans*) and development (*H. contortus*), leading to a *Str* phenotype at 100 μ M (like compound MMV1593539). The potent in vitro effect on the most pathogenic and reproductively active stage of *H. contortus* [66] encourages the optimisation of ABX464 via SAR studies and toxicity evaluation of analogues with increased potency. The quinoline scaffold of ABX464 (Figure 5) provides a sound pathway to medicinal chemistry optimisation with a wide range of diverse chemical changes possible [67]. A preliminary drug-likeness evaluation, using the Lipinski’s rule of five [68] as a guide, indicates that the ABX464 molecule fits three of four criteria; it contains one hydrogen bond donor, three hydrogen bond acceptors and has a molecular weight of 338.72 g/mol. Although the calculated logP is >5 (cLogP = 6.34; ChemDraw Ultra 12.0, PerkinElmer Informatics, Waltham, MA, USA), medicinal chemistry optimisation (by introducing hydrophilic functional groups) could address this issue. Furthermore, ABX464 analogues could be synthesised via a one-step nucleophilic aromatic substitution reaction, utilising quinoline- and/or aniline-derived building blocks. Such reagents are readily available at a relatively low cost, indicating that diverse ABX464 analogues could be produced cost-effectively and efficiently. Taken together, this information suggests that ABX464 is a promising candidate for optimisation as a nematocide.

ABX464 (i.e., MMV1581032) was first reported as a novel anti-HIV molecule [64] and is now undergoing phase 2 clinical trials as an anti-inflammatory compound for the treatment of ulcerative colitis, Crohn’s disease and rheumatoid arthritis of humans (cf. [ClinicalTrials.gov](https://clinicaltrials.gov), NIH; accessed on 15 September 2021). The anti-inflammatory properties of ABX464 are a consequence of RNA splicing-interference [65]. Campos et al. [64] showed that ABX464 binds to the human cap-binding complex (CBC), a protein structure located at the 5’-end of pre-mRNA transcript, which is required for efficient cellular and viral pre-mRNA splicing [64,65,69]. Upon ligand binding, CBC may undergo a conformational change, which markedly affects or alters pre-mRNA splicing [65]. As an anti-inflammatory, the binding of ABX464 to CBC has been shown to upregulate the non-coding micro-RNA, miR-124 [65,70]; miR-124 downregulates the secretion of several pro-inflammatory cytokines (IL-1 β , IL-6, TNF- α); thus, the ABX464-mediated upregulation of miR-124 likely inhibits inflammation [65,70]. Although the CBC appears to bind to all 7-methylguanylate-capped RNAs (such as pre-mRNA, mature mRNA or stable long non-coding RNAs; ref. [69]), ABX464 effects a specific upregulation of miR-124 transcription [65].

Currently, the mode/mechanism of action of ABX464 in nematodes is unknown, but could be explored using genomic, transcriptomic and/or proteomic methods. Genomic and transcriptomic approaches, similar to those employed for the discovery of the target of the anthelmintic monepantel [15,45,46,71–73], could be applicable to parasitic nematodes more broadly. For instance, utilising a forward genetic screen in *C. elegans*, Kaminsky et al. [71] established that the gene *acr-23* encoded a target of monepantel and then identified and validated its homologue in *H. contortus* (designated *mptl-1*) [72]. The potency of ABX464 in *C. elegans* suggests that such a functional genomic approach might be useful to study this compound’s target and mode of action [45,46]. It is also expected that the use of advanced proteomic tools, such as an affinity-based pulldown and/or cellular thermal shift assays plus mass spectrometry [74], should elucidate compound-target interaction(s), un-

derpinned by the knowledge of the somatic, excretory/secretory and phospho-proteomes for *H. contortus* [37,38,43]. Importantly, a combined, multi-omics approach is likely to be most effective towards the elucidation of mode(s) of action (cf. [40,45,46]). Although ABX464 presents as a promising candidate for mode of action studies, future work will prioritise the optimisation of this compound's nematocidal potency and the minimisation of toxicity on mammalian cells via an detailed SAR investigation.

4. Materials and Methods

4.1. Preparation of Compounds for Screening

The *Pandemic Response Box* compound library from MMV, Geneva, Switzerland, contains 400 structurally diverse, drug-like compounds (<https://www.mmv.org/mmv-open/pandemic-response-box/pandemic-response-box-supporting-information>; accessed on 15 September 2021). Individual compounds were supplied at concentrations of 10 mM or 2 mM in 10 µL of (100%) dimethyl sulfoxide (DMSO). Prior to screening, compounds were individually diluted to 40 µM in sterile Luria-Bertani broth (LB; cf. [31,75]). LB was autoclaved and supplemented with final concentrations of 100 IU/mL of penicillin, 100 µg/mL of streptomycin and 0.25 µg/mL of amphotericin B (Fungizone[®], cat. no. 15240-062, Gibco, Thermo Fisher Scientific, Waltham, MA, USA); this supplemented LB was designated LB*.

4.2. Production, Storage and Preparation of *H. contortus*

Haemonchus contortus (Haecon-5 strain; cf. [35]) was maintained in experimental sheep as described previously [35,76] and in accordance with the institutional animal ethics guidelines (permit no. 1714374; The University of Melbourne, Parkville, Victoria, Australia). Helminth-free Merino sheep (six months of age; male) were orally inoculated with 7000 third-stage larvae (L3s) of *H. contortus*. Four weeks after inoculation, faecal samples were collected from sheep with patent *H. contortus* infection. These samples were incubated at 27 °C and >90% relative humidity for one week to yield L3s [76], which were then collected in tap water and allowed to migrate through two layers of nylon mesh (pore size: 20 µm; Rowe Scientific, Doveton, Vic, Australia) to remove debris. Clean L3s were stored in the dark at 11 °C for up to six months [76]. Immediately prior to screening, *H. contortus* L3s were artificially exsheathed via exposure to 0.15% (*v/v*) sodium hypochlorite (NaOCl) for 20 min at 38 °C [76], achieving an exsheathment rate of 90%. The larvae were then immediately washed five times with 50 mL of sterile physiological saline solution by centrifugation at 500 × *g* (5 min) and resuspended in LB* at a concentration of 200 exsheathed L3s (xL3s) per 50 µL (for primary screen; see Section 4.4) or 300 xL3s per 50 µL (for dose-response assays; see Section 4.6).

Adult *H. contortus* were collected from the abomasa of sheep infected for 10 weeks, washed three times in phosphate-buffered saline (PBS; pH 7.4, 38 °C) and then three times in RPMI 1640 media supplemented with 4 mM L-glutamine, 100 U/mL of penicillin, 100 µg/mL of streptomycin and 0.25 µg/mL of amphotericin B (RPMI*, 38 °C; cat. no. 11875093, Thermo Fisher Scientific, Scoresby, Victoria, Australia). Using a dissecting microscope, female and male worms were separated in RPMI* (38 °C), and female worms immediately used (within ~1 h at 38 °C) to test compounds (see Section 4.8). Females were used because they produce large numbers (~4000) of eggs per day (cf. [77,78]), giving rise to the next generation of worms.

4.3. Production, Storage and Preparation of *C. elegans*

Caenorhabditis elegans (N2-wildtype Bristol strain) was maintained in the laboratory under standard conditions at 20 °C on nematode growth media (NGM) agar plates, with *Escherichia coli* OP50 as a food source [79]. Gravid adult worms were collected from NGM plates, washed with sterile M9 buffer and then treated with this buffer containing 0.4% (*v/v*) sodium hypochlorite and 170 mM sodium hydroxide for 4–8 min at 22–24 °C to release eggs [79,80]. The eggs were then washed five times with 15 mL of sterile M9 buffer (centrifugation at 500 × *g*, 2 min). After washing, the egg pellet was suspended in 8 mL of

M9 buffer in a 15 mL tube and gently agitated for 24 h at 22–24 °C (room temperature) to produce first-stage larvae (L1s); 45 h prior to screening, synchronised *C. elegans* L1s were inoculated on to NGM plates containing 500 µL of *E. coli* OP50 (~3000 larvae per plate) and allowed to develop to fourth-stage larvae (L4s) at 20 °C. L4s were collected from plates and washed twice with sterile M9 buffer by centrifugation (500 × *g*, 2 min) to remove *E. coli* OP50, and then resuspended in LB* at a concentration of 125 larvae per 50 µL (for primary screen; see Section 4.5) or 100 larvae per 50 µL (for dose-response assays; see Section 4.7).

4.4. Screening for Anthelmintic Activity against *H. contortus*

An established high-throughput phenotypic screening assay [31] was used to test the anthelmintic activity of compounds on *H. contortus* xL3s. Compounds were assessed for their effect on the motility of xL3s at a concentration of 20 µM in LB*. Four compounds, monepantel (Zolvix™; Elanco, Australia), monepantel/abamectin (Zolvix Plus™; Elanco, Australia), moxidectin (Cydectin®; Virbac, France) and compound MIPS-0018666 (abbreviated herein as M-666; cf. [81]), were used as positive controls (final concentration of 20 µM in LB*). Two solutions of LB* + 0.2% (*v/v*) DMSO and LB* + 1% (*v/v*) DMSO were used as negative controls. Test compounds as well as positive and negative controls were distributed amongst two flat-bottom 384-well microplates (cat no. 3680; Corning, Corning, NY, USA). Added to each well were 80 xL3s of *H. contortus* in 20 µL of LB* to give a final volume of 40 µL. Plates were then placed in a CO₂ incubator (10% [*v/v*] CO₂, 38 °C, >90% humidity; Forma, model no. 311, Thermo Fisher Scientific, Waltham, MA, USA). At 90 h, worm activity was captured using a WMicroTracker ONE unit (Phylumtech, Sunchales, Santa Fe, Argentina). Over a period of 15 min, disturbance of an infrared beam in individual wells was recorded as a worm ‘activity count’. Activity counts were then normalised to the positive and negative controls using the program Prism (v.9.1.0 GraphPad Software, San Diego, CA, USA) to remove plate-to-plate variation. The screening plates were then returned to the incubator (10% [*v/v*] CO₂, 38 °C, >90% humidity) for an additional three days to observe compound effects on larval development. At day seven, worms were fixed with 40 µL of Lugol’s solution (cat no. 62650; Sigma-Aldrich, St. Louis, MO, USA). Larval development was identified microscopically and recorded. Additionally, a compound that induced a non-wildtype phenotype (visible microscopically at 100-times magnification) in *H. contortus* worms was recorded. A compound that reduced xL3 motility by ≥70% and/or inhibited larval development or induced an abnormal phenotype (comparative to the negative control) was recorded as a ‘hit’ compound. The performance of the assay was monitored using the Z’-factor [82] calculated using data for the negative (DMSO) and positive (M-666) control compounds on individual plates.

4.5. Screening for Anthelmintic Activity against *C. elegans*

An established assay [83] was employed to test the anthelmintic activity of compounds on *C. elegans*. Compounds were assessed for their effect on the motility of worms at a concentration of 20 µM in LB*. Three compounds, monepantel, moxidectin and M-666 were used as positive controls (final concentration of 20 µM in LB*). Two solutions of LB* + 0.2% (*v/v*) DMSO and LB* + 1% (*v/v*) DMSO were used as negative controls. Test compounds and positive and negative controls were distributed amongst two flat-bottom 384-well microplates. Added to each well were 50 *C. elegans* in 20 µL of LB* to give a final volume of 40 µL. Plates were then placed in an incubator (Heratherm, model no. IMP180, Thermo Fisher Scientific, Waltham, MA, USA) at 20 °C for 40 h. At 40 h, the motility of *C. elegans* (in the transition from L4 to the adult stage) was captured using a WMicroTracker ONE unit. Over a period of 15 min, disturbance of an infrared beam in individual wells was recorded as a worm ‘activity count’. Activity counts were then normalised to the positive and negative controls using the program Prism v.9.1.0 to remove plate-to-plate variation. The screening plates were then returned to the incubator at 20 °C. At day 5, worms were fixed with 40 µL of Lugol’s solution. Any compound that induced a non-wildtype phenotype (viewed under microscope) in *C. elegans* worms was identified. A

compound that reduced worm motility by $\geq 70\%$ and/or induced an abnormal phenotype (comparative to the negative control) was recorded as a 'hit' compound. The Z' -factor was calculated in the same manner as in Section 4.4.

4.6. Dose-Response Assay Using *H. contortus*

An established dose-response assay [76] was employed to evaluate the potency of hit compounds against *H. contortus*. Test compounds were assessed individually for an effect on the motility of xL3s (18-point, 2-fold serial dilution in LB*, 100 μM to 7.6×10^{-4} μM). Two compounds, namely monepantel and moxidectin (prepared in the same manner as the test compounds), were used as positive controls. A solution of LB* + 0.25% (*v/v*) DMSO was used as a negative control. The test compounds and positive control compounds were arrayed in triplicate across individual flat-bottom 96-well microplates (cat. no. 3596; Corning, Corning, NY, USA), with six wells on each plate containing the negative control. Added to each well were 300 xL3s of *H. contortus* in 50 μL of LB* to give a final volume of 100 μL . Plates were then placed in a CO₂ incubator (10% [*v/v*] CO₂, 38 °C, >90% humidity). The motility of xL3s was measured (as a motility index, Mi) at 90 h, and larval development established at 168 h of incubation with compound, as described previously [76]. For individual wells, raw motility indices were then normalised with reference to the negative controls. The compound concentrations were log₁₀-transformed and fitted using a variable slope four-parameter equation, constraining the highest value to 100% using ordinary least squares fit model. The development inhibition and phenotypes of larvae were examined using a microscope [76], and results were analysed employing Prism v.9.1.0.

4.7. Dose-Response Assay Using *C. elegans*

A newly-established dose-response assay [83] was employed to further evaluate the potency of hit compounds against *C. elegans*. Test compounds were assessed individually for an effect on the motility of *C. elegans* (18-point, 2-fold serial dilution in LB*; from 100 μM to 7.6×10^{-4} μM) in the transition from the L4 to young adult stage. Two compounds, monepantel and moxidectin, were used as positive controls and prepared in the same manner as the test compounds. A solution of LB* + 0.25% (*v/v*) DMSO was used as a negative control. The test compounds and positive control compounds were arrayed in triplicate across individual flat-bottom 96-well microplates, with six wells on each plate containing the negative control. Added to each well were 100 *C. elegans* in 50 μL of LB* to give a final volume of 100 μL . Plates were then placed in an incubator at 20 °C for 40 h. At 40 h, worm activity was captured using a WMicroTracker ONE unit. Over a period of 15 min, disturbance of an infrared beam in individual wells was recorded as a worm activity count. Raw 'activity counts' for each well were normalised to the negative controls. The compound concentrations were log₁₀-transformed and fitted using a variable slope four-parameter equation, constraining the highest value to 100% using the ordinary least squares fit model employing Prism v.9.1.0.

4.8. Motility Assay against Adult Female *H. contortus*

A motility assay was employed to assess the *in vitro* activity of a compound (MMV1581032) on adult females of *H. contortus* using an established assay [29]. The compound was added in triplicate to the wells of a 24-well plate (cat. no. 3524; Corning, Corning, NY, USA) at a concentration of 100 μM in 500 μL of RPMI*. Two positive control compounds, monepantel and moxidectin, and a negative control containing 1% (*v/v*) DMSO only were included in triplicates on the same plate. Four adult females were added to each of the triplicate wells containing either the test compound or the controls and placed in a CO₂ incubator (10% [*v/v*] CO₂, 40 °C, >90% relative humidity) for 1 day. A video recording (30 sec) of each well was taken at 1 h, 2 h, 3 h, 5 h and 24 h during the total incubation period to assess the reduction in worm motility, which was scored as 3 ("good"), 2 ("low"), 1 ("very low") or 0 ("no movement"; cf. [29]). For each test or control compound,

the motility scores for each of the triplicate wells were calculated, normalised with reference to the negative control (100% motility) and recorded as a percentage.

4.9. Evaluation of Cellular and Mitochondrial Toxicities Using HepG2 Cells

A cell viability assay was employed to evaluate the cytotoxicity and mitotoxicity of one hit compound, MMV1581032, against HepG2 human hepatoma cells (Cat. no. 85011430; Sigma-Aldrich, St. Louis, MO, USA). The test compound was serially-diluted (7-point, 2-fold serial dilution, 100 μ M to 1.56 μ M) in Dulbecco's modified eagle medium (DMEM; with GlutaMax™ or 4 mM L-glutamine; cat. no. 10566016 or 11966025, respectively; Thermo Fisher Scientific, Waltham, MA, USA) supplemented with 25 mM D-glucose (cytotoxicity) or D-galactose (mitotoxicity), 10% inactivated foetal bovine serum (FBS), 100 IU/mL of penicillin, 100 μ g/mL of streptomycin and 0.25 μ g/mL of amphotericin B (denoted DMEM*). Monepantel and moxidectin (prepared in the same manner as the test compound) were included as positive control compounds. Two compounds, doxorubicin (cytotoxic; Sigma-Aldrich, St. Louis, MO, USA) and M-666 (mitotoxic; [81]), were used as positive controls at a single concentration of 10 μ M. A solution of DMEM* + 0.25% (v/v) DMSO was used as a negative control. HepG2 cells were seeded into wells of a 96-well plate in 80 μ L of DMEM* (at 5.5×10^4 cells per well) and allowed to adhere for 16 h at 37 °C and 5% (v/v) CO₂ at >90% humidity prior to incubation with individual compounds, at a final volume of 100 μ L. For the assessment of mitochondrial toxicity, cells were starved of serum (DMEM* without FBS) for 4 h prior to the incubation with individual compounds [84,85]. Following 48 h of incubation, cell viability was determined by crystal violet staining [86]. The absorbance (595 nm) of treated cells was normalised using the negative controls (viability: 100%) to calculate the cell viability. All compounds and controls were tested in triplicate. To determine the half-maximal cytotoxic concentration (CC₅₀) and half-maximal mitotoxic concentration (MC₅₀) values, compound concentrations were log₁₀-transformed, baseline-corrected using a respective positive control (doxorubicin or M-666) and fitted using a variable slope four-parameter equation employing the ordinary least squares fit model using Prism v.9.1.0.

Author Contributions: Conceptualization, R.B.G. and H.T.S.; methodology, A.C.T.; validation, H.T.S. and A.C.T.; formal analysis, H.T.S. and A.C.T.; investigation, H.T.S., A.C.T. and J.J.B.; resources, R.B.G., A.C.T., B.E.S. and A.J.; writing—original draft preparation, H.T.S. and R.B.G.; writing—review and editing, H.T.S., A.C.T., J.J.B., A.J., T.N.C.W., K.S., P.R.B., N.N., B.E.S. and R.B.G.; visualisation, H.T.S.; supervision, R.B.G., B.E.S. and A.C.T.; project administration, R.B.G. and A.C.T.; funding acquisition, R.B.G., A.J. and B.E.S. All authors have read and agreed to the published version of the manuscript.

Funding: This research was funded by the Australian Research Council (ARC, LP190101209) and Phylumtech (Argentina).

Institutional Review Board Statement: This study was conducted in accordance with the institutional animal ethics guidelines (permit no. 1714374; The University of Melbourne).

Informed Consent Statement: Not applicable.

Data Availability Statement: Data is contained within the article.

Acknowledgments: We are grateful to Anna Sulakova and the team at Medicines for Malaria Venture (MMV) for curating and supplying the *Pandemic Response Box*, and for their ongoing support.

Conflicts of Interest: The authors declare no conflict of interest. The funders had no role in the design of the study; in the collection, analyses or interpretation of data; in the writing of the manuscript, or in the decision to publish the results.

References

1. Fenwick, A. The global burden of neglected tropical diseases. *Public Health* **2012**, *126*, 233–236. [[CrossRef](#)] [[PubMed](#)]
2. Fitzpatrick, J.L. Global food security: The impact of veterinary parasites and parasitologists. *Vet. Parasitol.* **2013**, *195*, 233–248. [[CrossRef](#)] [[PubMed](#)]
3. Casulli, A. New global targets for NTDs in the WHO roadmap 2021–2030. *PLoS Negl. Trop. Dis.* **2021**, *15*, e0009373. [[CrossRef](#)]

4. Roeber, F.; Jex, A.R.; Gasser, R.B. Impact of gastrointestinal parasitic nematodes of sheep, and the role of advanced molecular tools for exploring epidemiology and drug resistance—An Australian perspective. *Parasit. Vectors* **2013**, *6*, 153. [[CrossRef](#)] [[PubMed](#)]
5. Le Jambre, L.F. Relationship of blood loss to worm numbers, biomass and egg production in *Haemonchus* infected sheep. *Int. J. Parasitol.* **1995**, *25*, 269–273. [[CrossRef](#)]
6. Besier, R.B.; Kahn, L.P.; Sargison, N.D.; Van Wyk, J.A. Diagnosis, treatment and management of *Haemonchus contortus* in small ruminants. *Adv. Parasitol.* **2016**, *93*, 181–238. [[CrossRef](#)] [[PubMed](#)]
7. Veglia, F. The Anatomy and Life-History of *Haemonchus contortus* (Rud). *Rep. Dir. Vet. Res.* **1915**, 3–4, 347–500.
8. Kearney, P.E.; Murray, P.J.; Hoy, J.M.; Hohenhaus, M.; Kotze, A. The “toolbox” of strategies for managing *Haemonchus contortus* in goats: What’s in and what’s out. *Vet. Parasitol.* **2016**, *220*, 93–107. [[CrossRef](#)]
9. Lanusse, C.E.; Alvarez, L.I.; Lifschitz, A.L. Gaining insights into the pharmacology of anthelmintics using *Haemonchus contortus* as a model nematode. *Adv. Parasitol.* **2016**, *93*, 465–518. [[CrossRef](#)]
10. Sargison, N.D. Pharmaceutical treatments of gastrointestinal nematode infections of sheep—future of anthelmintic drugs. *Vet. Parasitol.* **2012**, *189*, 79–84. [[CrossRef](#)]
11. Kotze, A.C.; Prichard, R.K. Anthelmintic resistance in *Haemonchus contortus*: History, mechanisms and diagnosis. *Adv. Parasitol.* **2016**, *93*, 397–428. [[CrossRef](#)]
12. Waller, P.J. Global perspectives on nematode parasite control in ruminant livestock: The need to adopt alternatives to chemotherapy, with emphasis on biological control. *Anim. Health Res. Rev.* **2003**, *4*, 35–43. [[CrossRef](#)] [[PubMed](#)]
13. Sargison, N.D. Keys to solving health problems in small ruminants: Anthelmintic resistance as a threat to sustainable nematode control. *Small Rumin. Res.* **2016**, *142*, 11–15. [[CrossRef](#)]
14. Papadopoulos, E. Anthelmintic resistance in sheep nematodes. *Small Rumin. Res.* **2008**, *76*, 99–103. [[CrossRef](#)]
15. Kaminsky, R.; Gauvry, N.; Schorderet Weber, S.; Skripsky, T.; Bouvier, J.; Wenger, A.; Schroeder, F.; Desaulles, Y.; Hotz, R.; Goebel, T.; et al. identification of the amino-acetonitrile derivative monepantel (AAD 1566) as a new anthelmintic drug development candidate. *Parasitol. Res.* **2008**, *103*, 931–939. [[CrossRef](#)] [[PubMed](#)]
16. Lee, B.H.; Clothier, M.F.; Dutton, F.E.; Nelson, S.J.; Johnson, S.S.; Thompson, D.P.; Geary, T.G.; Whaley, H.D.; Haber, C.L.; Marshall, V.P.; et al. Marcfortine and paraherquamide class of anthelmintics: Discovery of PNU-141962. *Curr. Top. Med. Chem.* **2002**, *2*, 779–793. [[CrossRef](#)] [[PubMed](#)]
17. Little, P.R.; Hodges, A.; Watson, T.G.; Seed, J.A.; Maeder, S.J. Field efficacy and safety of an oral formulation of the novel combination anthelmintic, derquantel-abamectin, in sheep in New Zealand. *N. Z. Vet. J.* **2010**, *58*, 121–129. [[CrossRef](#)] [[PubMed](#)]
18. Jiao, Y.; Preston, S.; Hofmann, A.; Taki, A.; Baell, J.; Chang, B.C.H.; Jabbar, A.; Gasser, R.B. A perspective on the discovery of selected compounds with anthelmintic activity against the barber’s pole worm—where to from here? *Adv. Parasitol.* **2020**, *108*, 1–45. [[CrossRef](#)]
19. Herath, H.M.P.D.; Taki, A.C.; Sleebs, B.E.; Hofmann, A.; Nguyen, N.; Preston, S.; Davis, R.A.; Jabbar, A.; Gasser, R.B. Advances in the discovery and development of anthelmintics by harnessing natural product scaffolds. *Adv. Parasitol.* **2021**, *111*, 203–251. [[CrossRef](#)]
20. Camp, D.; Newman, S.; Pham, N.B.; Quinn, R.J. Nature Bank and the Queensland compound library: Unique international resources at the Eskitis Institute for Drug Discovery. *Comb. Chem. High Throughput Screen.* **2014**, *17*, 201–209. [[CrossRef](#)]
21. Preston, S.; Jiao, Y.; Jabbar, A.; McGee, S.L.; Laleu, B.; Willis, P.; Wells, T.N.C.; Gasser, R.B. Screening of the “Pathogen Box” identifies an approved pesticide with major anthelmintic activity against the barber’s pole worm. *Int. J. Parasitol. Drugs Drug Resist.* **2016**, *6*, 329–334. [[CrossRef](#)] [[PubMed](#)]
22. Herath, H.M.P.D.; Preston, S.; Hofmann, A.; Davis, R.A.; Koehler, A.V.; Chang, B.C.H.; Jabbar, A.; Gasser, R.B. Screening of a small, well-curated natural product-based library identifies two rotenoids with potent nematocidal activity against *Haemonchus contortus*. *Vet. Parasitol.* **2017**, *244*, 172–175. [[CrossRef](#)] [[PubMed](#)]
23. Jiao, Y.; Preston, S.; Song, H.; Jabbar, A.; Liu, Y.; Baell, J.; Hofmann, A.; Hutchinson, D.; Wang, T.; Koehler, A.V.; et al. Assessing the anthelmintic activity of pyrazole-5-carboxamide derivatives against *Haemonchus contortus*. *Parasit. Vectors* **2017**, *10*, 272. [[CrossRef](#)] [[PubMed](#)]
24. Jiao, Y.; Preston, S.; Koehler, A.V.; Stroehlein, A.J.; Chang, B.C.H.; Simpson, K.J.; Cowley, K.J.; Palmer, M.J.; Laleu, B.; Wells, T.N.C.; et al. Screening of the ‘Stasis Box’ identifies two kinase inhibitors under pharmaceutical development with activity against *Haemonchus contortus*. *Parasit. Vectors* **2017**, *10*, 323. [[CrossRef](#)] [[PubMed](#)]
25. Preston, S.; Jiao, Y.; Baell, J.B.; Keiser, J.; Crawford, S.; Koehler, A.V.; Wang, T.; Simpson, M.M.; Kaplan, R.M.; Cowley, K.J.; et al. Screening of the ‘Open Scaffolds’ collection from compounds Australia identifies a new chemical entity with anthelmintic activities against different developmental stages of the barber’s pole worm and other parasitic nematodes. *Int. J. Parasitol. Drugs Drug Resist.* **2017**, *7*, 286–294. [[CrossRef](#)] [[PubMed](#)]
26. Herath, H.M.P.D.; Song, H.; Preston, S.; Jabbar, A.; Wang, T.; McGee, S.L.; Hofmann, A.; Garcia-Bustos, J.; Chang, B.C.H.; Koehler, A.V.; et al. Arylpyrrole and fipronil analogues that inhibit the motility and/or development of *Haemonchus contortus* in vitro. *Int. J. Parasitol. Drugs Drug Resist.* **2018**, *8*, 379–385. [[CrossRef](#)] [[PubMed](#)]
27. Jiao, Y.; Preston, S.; Garcia-Bustos, J.F.; Baell, J.B.; Ventura, S.; Le, T.; McNamara, N.; Nguyen, N.; Botteon, A.; Skinner, C.; et al. Tetrahydroquinoxalines induce a lethal evisceration phenotype in *Haemonchus contortus* in vitro. *Int. J. Parasitol. Drugs Drug Resist.* **2019**, *9*, 59–71. [[CrossRef](#)]

28. Nguyen, L.T.; Kurz, T.; Preston, S.; Brueckmann, H.; Lungerich, B.; Herath, H.M.P.D.; Koehler, A.V.; Wang, T.; Skálová, L.; Jabbar, A.; et al. Phenotypic screening of the ‘Kurz-box’ of chemicals identifies two compounds (BLK127 and HBK4) with anthelmintic activity in vitro against parasitic larval stages of *Haemonchus contortus*. *Parasit. Vectors* **2019**, *12*, 191. [[CrossRef](#)]
29. Taki, A.C.; Brkljača, R.; Wang, T.; Koehler, A.V.; Ma, G.; Danne, J.; Ellis, S.; Hofmann, A.; Chang, B.C.H.; Jabbar, A.; et al. Natural compounds from the marine brown alga *Caulocystis cephalornithos* with potent in vitro-activity against the parasitic nematode *Haemonchus contortus*. *Pathogens* **2020**, *9*, 550. [[CrossRef](#)]
30. Taki, A.C.; Jabbar, A.; Kurz, T.; Lungerich, B.; Ma, G.; Byrne, J.J.; Pflieger, M.; Asfaha, Y.; Fischer, F.; Chang, B.C.H.; et al. Three small molecule entities (MPK18, MPK334 and YAK308) with activity against *Haemonchus contortus* in vitro. *Molecules* **2021**, *26*, 2819. [[CrossRef](#)]
31. Taki, A.C.; Byrne, J.J.; Wang, T.; Sleebs, B.E.; Nguyen, N.; Hall, R.S.; Korhonen, P.K.; Chang, B.C.H.; Jackson, P.; Jabbar, A.; et al. High-throughput phenotypic assay to screen for anthelmintic activity on *Haemonchus contortus*. *Pharmaceuticals* **2021**, *14*, 616. [[CrossRef](#)] [[PubMed](#)]
32. Le, T.G.; Kundu, A.; Ghoshal, A.; Nguyen, N.H.; Preston, S.; Jiao, Y.; Ruan, B.; Xue, L.; Huang, F.; Keiser, J.; et al. Structure-activity relationship studies of tolfenpyrad reveal subnanomolar inhibitors of *Haemonchus contortus* development. *J. Med. Chem.* **2019**, *62*, 1036–1053. [[CrossRef](#)] [[PubMed](#)]
33. Le, T.G.; Kundu, A.; Ghoshal, A.; Nguyen, N.H.; Preston, S.; Jiao, Y.; Ruan, B.; Xue, L.; Huang, F.; Keiser, J.; et al. Novel 1-methyl-1h-pyrazole-5-carboxamide derivatives with potent anthelmintic activity. *J. Med. Chem.* **2019**, *62*, 3367–3380. [[CrossRef](#)] [[PubMed](#)]
34. Laing, R.; Kikuchi, T.; Martinelli, A.; Tsai, I.J.; Beech, R.N.; Redman, E.; Holroyd, N.; Bartley, D.J.; Beasley, H.; Britton, C.; et al. The genome and transcriptome of *Haemonchus contortus*, a key model parasite for drug and vaccine discovery. *Genome Biol.* **2013**, *14*, R88. [[CrossRef](#)] [[PubMed](#)]
35. Schwarz, E.M.; Korhonen, P.K.; Campbell, B.E.; Young, N.D.; Jex, A.R.; Jabbar, A.; Hall, R.S.; Mondal, A.; Howe, A.C.; Pell, J.; et al. The genome and developmental transcriptome of the strongylid nematode *Haemonchus contortus*. *Genome Biol.* **2013**, *14*, R89. [[CrossRef](#)]
36. Wang, T.; Nie, S.; Ma, G.; Korhonen, P.K.; Koehler, A.V.; Ang, C.-S.; Reid, G.E.; Williamson, N.A.; Gasser, R.B. The developmental lipidome of *Haemonchus contortus*. *Int. J. Parasitol.* **2018**, *48*, 887–895. [[CrossRef](#)]
37. Wang, T.; Ma, G.; Ang, C.-S.; Korhonen, P.K.; Koehler, A.V.; Young, N.D.; Nie, S.; Williamson, N.A.; Gasser, R.B. High throughput LC-MS/MS-based proteomic analysis of excretory-secretory products from short-term in vitro culture of *Haemonchus contortus*. *J. Proteom.* **2019**, *204*, 103375. [[CrossRef](#)]
38. Wang, T.; Ma, G.; Ang, C.-S.; Korhonen, P.K.; Xu, R.; Nie, S.; Koehler, A.V.; Simpson, R.J.; Greening, D.W.; Reid, G.E.; et al. Somatic proteome of *Haemonchus contortus*. *Int. J. Parasitol.* **2019**, *49*, 311–320. [[CrossRef](#)]
39. Doyle, S.R.; Tracey, A.; Laing, R.; Holroyd, N.; Bartley, D.; Bazant, W.; Beasley, H.; Beech, R.; Britton, C.; Brooks, K.; et al. Genomic and transcriptomic variation defines the chromosome-scale assembly of *Haemonchus contortus*, a model gastrointestinal worm. *Commun. Biol.* **2020**, *3*, 1–16. [[CrossRef](#)]
40. Ma, G.; Gasser, R.B.; Wang, T.; Korhonen, P.K.; Young, N.D. Toward integrative ‘omics of the barber’s pole worm and related parasitic nematodes. *Infect. Genet. Evol.* **2020**, *85*, 104500. [[CrossRef](#)]
41. Ma, G.; Wang, T.; Korhonen, P.K.; Hofmann, A.; Sternberg, P.W.; Young, N.D.; Gasser, R.B. Elucidating the molecular and developmental biology of parasitic nematodes: Moving to a multiomics paradigm. *Adv. Parasitol.* **2020**, *108*, 175–229. [[CrossRef](#)] [[PubMed](#)]
42. Wang, T.; Gasser, R.B. Prospects of using high-throughput proteomics to underpin the discovery of animal host–nematode interactions. *Pathogens* **2021**, *10*, 825. [[CrossRef](#)] [[PubMed](#)]
43. Wang, T.; Ma, G.; Ang, C.-S.; Korhonen, P.K.; Stroehlein, A.J.; Young, N.D.; Hofmann, A.; Chang, B.C.H.; Williamson, N.A.; Gasser, R.B. The developmental phosphoproteome of *Haemonchus contortus*. *J. Proteom.* **2020**, *213*, 103615. [[CrossRef](#)] [[PubMed](#)]
44. Holden-Dye, L.; Walker, R.J. Anthelmintic drugs and nematicides: Studies in *Caenorhabditis elegans*. In *WormBook: The Online Review of C. elegans Biology*; The C. elegans Research Community: Pasadena, CA, USA, 2014; pp. 1–29.
45. Hahnel, S.R.; Dilks, C.M.; Heisler, I.; Andersen, E.C.; Kulke, D. *Caenorhabditis elegans* in anthelmintic research—Old model, new perspectives. *Int. J. Parasitol. Drugs Drug Resist.* **2020**, *14*, 237–248. [[CrossRef](#)]
46. Sepúlveda-Crespo, D.; Reguera, R.M.; Rojo-Vázquez, F.; Balaña-Fouce, R.; Martínez-Valladares, M. drug discovery technologies: *Caenorhabditis elegans* as a model for anthelmintic therapeutics. *Med. Res. Rev.* **2020**, *40*, 1715–1753. [[CrossRef](#)] [[PubMed](#)]
47. Harris, T.W.; Arnaboldi, V.; Cain, S.; Chan, J.; Chen, W.J.; Cho, J.; Davis, P.; Gao, S.; Grove, C.A.; Kishore, R.; et al. WormBase: A modern model organism information resource. *Nucleic Acids Res.* **2020**, *48*, D762–D767. [[CrossRef](#)]
48. Gasser, R.B.; Schwarz, E.M.; Korhonen, P.K.; Young, N.D. Understanding *Haemonchus contortus* better through genomics and transcriptomics. *Adv. Parasitol.* **2016**, *93*, 519–567. [[CrossRef](#)]
49. Herath, H.M.P.D.; Preston, S.; Jabbar, A.; Garcia-Bustos, J.; Addison, R.S.; Hayes, S.; Rali, T.; Wang, T.; Koehler, A.V.; Chang, B.C.H.; et al. Selected α -pyrones from the plants *Cryptocarya novoguineensis* (Lauraceae) and *Piper methysticum* (Piperaceae) with activity against *Haemonchus contortus* in vitro. *Int. J. Parasitol. Drugs Drug Resist.* **2019**, *9*, 72–79. [[CrossRef](#)]
50. Zoraghi, R.; Campbell, S.; Kim, C.; Dullaghan, E.M.; Blair, L.M.; Gillard, R.M.; Reiner, N.E.; Sperry, J. Discovery of a 1,2-bis(3-indolyl)ethane that selectively inhibits the pyruvate kinase of methicillin-resistant *Staphylococcus aureus* over human isoforms. *Bioorg. Med. Chem. Lett.* **2014**, *24*, 5059–5062. [[CrossRef](#)]

51. Palaima, E.; Leymarie, N.; Stroud, D.; Mizanur, R.M.; Hodgkin, J.; Gravato-Nobre, M.J.; Costello, C.E.; Cipollo, J.F. The *Caenorhabditis elegans* bus-2 mutant reveals a new class of O-glycans affecting bacterial resistance. *J. Biol. Chem.* **2010**, *285*, 17662–17672. [[CrossRef](#)]
52. Hubbard, T.D.; Murray, I.A.; Perdew, G.H. Indole and tryptophan metabolism: Endogenous and dietary routes to Ah receptor activation. *Drug Metab. Dispos.* **2015**, *43*, 1522–1535. [[CrossRef](#)] [[PubMed](#)]
53. Nepali, K.; Lee, H.-Y.; Liou, J.-P. Nitro-group-containing drugs. *J. Med. Chem.* **2019**, *62*, 2851–2893. [[CrossRef](#)] [[PubMed](#)]
54. Chackalamannil, S.; Wang, Y.; Greenlee, W.J.; Hu, Z.; Xia, Y.; Ahn, H.-S.; Boykow, G.; Hsieh, Y.; Palamanda, J.; Agans-Fantuzzi, J.; et al. Discovery of a novel, orally active himbacine-based thrombin receptor antagonist (sCH 530348) with potent antiplatelet activity. *J. Med. Chem.* **2008**, *51*, 3061–3064. [[CrossRef](#)] [[PubMed](#)]
55. Gryka, R.J.; Buckley, L.F.; Anderson, S.M. Vorapaxar: The current role and future directions of a novel protease-activated receptor antagonist for risk reduction in atherosclerotic disease. *Drugs R&D* **2017**, *17*, 65–72. [[CrossRef](#)]
56. Malaska, M.J.; Fauq, A.H.; Kozikowski, A.P.; Aagaard, P.J.; McKinney, M. Chemical modification of ring C of himbacine: Discovery of a pharmacophoric element for M2-selectivity. *Bioorg. Med. Chem. Lett.* **1995**, *5*, 61–66. [[CrossRef](#)]
57. Chackalamannil, S.; Doller, D.; McQuade, R.; Ruperto, V. Himbacine analogs as muscarinic receptor antagonists—Effects of tether and heterocyclic variations. *Bioorg. Med. Chem. Lett.* **2004**, *14*, 3967–3970. [[CrossRef](#)]
58. Steger, K.A.; Avery, L. The GAR-3 muscarinic receptor cooperates with calcium signals to regulate muscle contraction in the *Caenorhabditis elegans* pharynx. *Genetics* **2004**, *167*, 633–643. [[CrossRef](#)]
59. Blaxter, M.L.; De Ley, P.; Garey, J.R.; Liu, L.X.; Scheldeman, P.; Vierstraete, A.; Vanfleteren, J.R.; Mackey, L.Y.; Dorris, M.; Frisse, L.M.; et al. A molecular evolutionary framework for the phylum Nematoda. *Nature* **1998**, *392*, 71–75. [[CrossRef](#)]
60. Smythe, A.B.; Holovachov, O.; Kocot, K.M. Improved phylogenomic sampling of free-living nematodes enhances resolution of higher-level nematode phylogeny. *BMC Evol. Biol.* **2019**, *19*, 121. [[CrossRef](#)]
61. Chackalamannil, S.; Davies, R.J.; Asberom, T.; Doller, D.; Leone, D. A highly efficient total synthesis of (+)-himbacine. *J. Am. Chem. Soc.* **1996**, *118*, 9812–9813. [[CrossRef](#)]
62. Chackalamannil, S.; Davies, R.J.; Wang, Y.; Asberom, T.; Doller, D.; Wong, J.; Leone, D.; McPhail, A.T. Total synthesis of (+)-himbacine and (+)-himbeline. *J. Org. Chem.* **1999**, *64*, 1932–1940. [[CrossRef](#)] [[PubMed](#)]
63. Clasby, M.C.; Chackalamannil, S.; Czarniecki, M.; Doller, D.; Eagen, K.; Greenlee, W.; Kao, G.; Lin, Y.; Tsai, H.; Xia, Y.; et al. Metabolism-identified identification of a potent thrombin receptor antagonist. *J. Med. Chem.* **2007**, *50*, 129–138. [[CrossRef](#)] [[PubMed](#)]
64. Campos, N.; Myburgh, R.; Garcel, A.; Vautrin, A.; Lapasset, L.; Nadal, E.S.; Mahuteau-Betzer, F.; Najman, R.; Fornarelli, P.; Tantale, K.; et al. Long lasting control of viral rebound with a new drug ABX464 targeting Rev—Mediated viral RNA biogenesis. *Retrovirology* **2015**, *12*, 30. [[CrossRef](#)] [[PubMed](#)]
65. Vautrin, A.; Manchon, L.; Garcel, A.; Campos, N.; Lapasset, L.; Laaref, A.M.; Bruno, R.; Gislard, M.; Dubois, E.; Scherrer, D.; et al. Both anti-inflammatory and antiviral properties of novel drug candidate ABX464 are mediated by modulation of RNA splicing. *Sci. Rep.* **2019**, *9*, 792. [[CrossRef](#)] [[PubMed](#)]
66. Besier, R.B.; Kahn, L.P.; Sargison, N.D.; Van Wyk, J.A. The pathophysiology, ecology and epidemiology of *Haemonchus contortus* infection in small ruminants. *Adv. Parasitol.* **2016**, *93*, 95–143. [[CrossRef](#)] [[PubMed](#)]
67. Senerovic, L.; Opsenica, D.; Moric, I.; Aleksic, I.; Spasić, M.; Vasiljevic, B. Quinolines and quinolones as antibacterial, antifungal, anti-virulence, antiviral and anti-parasitic agents. In *Advances in Microbiology, Infectious Diseases and Public Health, Advances in Experimental Medicine and Biology*; Donelli, G., Ed.; Springer International Publishing: Cham, Switzerland, 2019; Volume 1282, pp. 37–69. ISBN 978-3-030-53647-3.
68. Lipinski, C.A.; Lombardo, F.; Dominy, B.W.; Feeney, P.J. Experimental and computational approaches to estimate solubility and permeability in drug discovery and development settings. *Adv. Drug Deliv. Rev.* **1997**, *23*, 3–25. [[CrossRef](#)]
69. Gonatopoulos-Pournatzis, T.; Cowling, V.H. Cap-binding complex (CBC). *Biochem. J.* **2014**, *457*, 231–242. [[CrossRef](#)]
70. Tazi, J.; Begon-Pescia, C.; Campos, N.; Apolit, C.; Garcel, A.; Scherrer, D. Specific and selective induction of miR-124 in immune cells by the quinoline ABX464: A transformative therapy for inflammatory diseases. *Drug Discov. Today* **2020**, *26*, 1030–1039. [[CrossRef](#)]
71. Kaminsky, R.; Ducray, P.; Jung, M.; Clover, R.; Rufener, L.; Bouvier, J.; Weber, S.S.; Wenger, A.; Wieland-Berghausen, S.; Goebel, T.; et al. A new class of anthelmintics effective against drug-resistant nematodes. *Nature* **2008**, *452*, 176–180. [[CrossRef](#)]
72. Rufener, L.; Mäser, P.; Roditi, I.; Kaminsky, R. *Haemonchus contortus* acetylcholine receptors of the DEG-3 subfamily and their role in sensitivity to monepantel. *PLoS Pathog.* **2009**, *5*, e1000380. [[CrossRef](#)]
73. Gilleard, J.S. *Haemonchus contortus* as a paradigm and model to study anthelmintic drug resistance. *Parasitology* **2013**, *140*, 1506–1522. [[CrossRef](#)]
74. Friman, T. Mass spectrometry-based cellular thermal shift assay (CETSA[®]) for target deconvolution in phenotypic drug discovery. *Bioorg. Med. Chem.* **2020**, *28*, 115174. [[CrossRef](#)] [[PubMed](#)]
75. Bertani, G. Studies on lysogenesis. I. The mode of phage liberation by lysogenic *Escherichia coli*. *J. Bacteriol.* **1951**, *62*, 293–300. [[CrossRef](#)] [[PubMed](#)]
76. Preston, S.; Jabbar, A.; Nowell, C.; Joachim, A.; Rutkowski, B.; Baell, J.; Cardno, T.; Korhonen, P.K.; Piedrafita, D.; Ansell, B.R.E.; et al. Low cost whole-organism screening of compounds for anthelmintic activity. *Int. J. Parasitol.* **2015**, *45*, 333–343. [[CrossRef](#)] [[PubMed](#)]

77. Fleming, M.W. Size of inoculum dose regulates in part worm burdens, fecundity, and lengths in ovine *Haemonchus contortus* infections. *J. Parasitol.* **1988**, *74*, 975–978. [[CrossRef](#)] [[PubMed](#)]
78. Coyne, M.J.; Smith, G. The mortality and fecundity of *Haemonchus contortus* in parasite-naive and parasite-exposed sheep following single experimental infections. *Int. J. Parasitol.* **1992**, *22*, 315–325. [[CrossRef](#)]
79. Stiernagle, T. Maintenance of *C. elegans*. In *WormBook: The Online Review of C. elegans Biology*; The *C. elegans* Research Community: Pasadena, CA, USA, 2006; pp. 1–11.
80. Porta-de-la-Riva, M.; Fontrodona, L.; Villanueva, A.; Cerón, J. Basic *Caenorhabditis elegans* methods: Synchronization and observation. *J. Vis. Exp.* **2012**, *64*, e4019. [[CrossRef](#)]
81. Le, T.G.; Kundu, A.; Ghoshal, A.; Nguyen, N.H.; Preston, S.; Jiao, Y.; Ruan, B.; Xue, L.; Huang, F.; Keiser, J.; et al. Optimization of novel 1-methyl-1 h-pyrazole-5-carboxamides leads to high potency larval development inhibitors of the barber's pole worm. *J. Med. Chem.* **2018**, *61*, 10875–10894. [[CrossRef](#)]
82. Zhang, J.-H.; Chung, T.D.Y.; Oldenburg, K.R. A simple statistical parameter for use in evaluation and validation of high throughput screening assays. *J. Biomol. Screen.* **1999**, *4*, 67–73. [[CrossRef](#)]
83. Taki, A.C.; Byrne, J.J.; Boag, P.R.; Jabbar, A.; Gasser, R.B. Practical high-throughput method to screen compounds for anthelmintic activity against *Caenorhabditis elegans*. *Molecules* **2021**, *26*, 4156. [[CrossRef](#)]
84. Swiss, R.L.; Will, Y. Assessment of mitochondrial toxicity in HepG2 cells cultured in high-glucose- or galactose-containing media. *Curr. Protoc. Toxicol.* **2011**, *49*, 2.20.1–2.20.14.
85. Kamalian, L.; Chadwick, A.E.; Bayliss, M.; French, N.S.; Monshouwer, M.; Snoeys, J.; Park, B.K. The utility of HepG2 cells to identify direct mitochondrial dysfunction in the absence of cell death. *Toxicol. In Vitro* **2015**, *29*, 732–740. [[CrossRef](#)] [[PubMed](#)]
86. Śliwka, L.; Wiktorska, K.; Suchocki, P.; Milczarek, M.; Mielczarek, S.; Lubelska, K.; Cierpień, T.; Łyzwa, P.; Kielbasiński, P.; Jaromin, A.; et al. The comparison of MTT and CVS assays for the assessment of anticancer agent interactions. *PLoS ONE* **2016**, *11*, e0155772. [[CrossRef](#)] [[PubMed](#)]